

# Development of Mid-IR Fiber Bundle for Thermal Imaging

Andrea Ventura, Joris Lousteau, Fedia Ben Slimen, Nicholas White and Francesco Poletti  
*Optoelectronics Research Centre, University of Southampton, Southampton, SO17 1TW, U.K.*

**Keywords:** Thermal Imaging, Infrared Fibers, Coherent Bundle, Modelling.

**Abstract:** We present and discuss the fabrication and characterization of a Mid-Infrared (Mid-IR) transparent flexible bundle based on 1200 fibers whose cores consist of a  $\text{Ge}_{30}\text{As}_{13}\text{Se}_{32}\text{Te}_{25}$  chalcogenide glass and the cladding of a Fluorinated Ethylene Propylene (FEP). The Mid-IR fiber bundle was manufactured using the stack and draw method. The high index contrast between the glass and the cladding allows for strong field confinement of the well guided modes within the chalcogenide glass core transparent across the Mid-IR. Higher order modes, which could be prone to cross talk, suffered high losses thanks to the high attenuation offered by the polymer cladding. Additionally, the FEP cladding confers the bundle mechanical flexibility. Following a qualitative thermal imaging assessment, we also present and discuss the experimental loss measurements of the fiber bundle and we compare them to values obtained through modelling to conclude on the potential prospect of the manufactured bundle and its possible improvements.

## 1 INTRODUCTION

Over the last two decades, Mid-IR detector technology and other Mid-IR optical components such as lens and material have undergone significant development and improvement in terms of performance and reliability. Thermal imaging is now slowly becoming a standard inspection technique in fields such as defence, security, industrial processes, medical and physiological activities monitoring. Thermal imaging relies on the detection of infrared radiation (IR) emitted by any physical body held at a temperature above 0 K. Mid-IR detectors based either on InSb technology or on the Microbolometer detectors offer high sensitivity/detectivity in the Mid-IR region (1-5.5  $\mu\text{m}$ ) and in the wavelength range between 8-14  $\mu\text{m}$ , respectively (Infrared Detectors, 2017). In some cases the main restriction to a widespread use of thermal imaging is the lack of a flexible imaging bundle for the inspection of remote access area or purely for its practicality and convenience. Although a boroscope approach is achievable, a Mid-IR transmitting coherent fiber bundle is the most adapted solution thanks to its flexibility. “Coherent” fiber bundle consists in arrays of optical fibers where each fiber represents a pixel, where “coherent” implies a direct pixel matching between the bundle ends. If compared to boroscope approach the fiber bundle is insensitive to vibrations

due to the absence of moving optics and allows to change the viewing angle quickly. Despite its technological importance there are currently no infrared high resolution fiber bundles commercially available. In order to realise a coherent fiber bundle that operates in the Mid-IR region, both the bundle material and the bundle structure play an important role. Numerous attempts were made to develop such device (Rave, 2000; Gopal, 2004; Zhang, 2015; Chenard, 2017; Nishii, 1991). These works involved different Mid-IR transmitting materials and hollow core fiber structure. Perhaps the most significant work reported in terms of performances is that of Nishii *et al.* (1991). Although, the final bundle appears to be bulky and not fully coherent, Nishii *et al.* (1991) demonstrated a high spatial resolution bundle for temperatures low as 25 °C. The objective of this work is to develop a coherent fiber bundle a few meters long with low loss, high spatial resolution and efficient for temperatures between 20 and 200 °C. As mentioned before, in the literature different Mid-IR fiber bundles have been reported, but they still have limitations such as size, resolution, high losses and flexibility. We present the fabrication of a coherent Mid-IR fiber bundle whereby by exploiting a pertinent choice of materials we aimed at reducing the pixel and the pitch dimensions without inducing a severe crosstalk.

## 2 BUNDLE FABRICATION AND CHARACTERIZATION

We designed and chose the materials for manufacturing the Mid-IR transmitting bundle according to the following general guideline. The core material must have:

- Transparency in the Mid-IR region (2-20  $\mu\text{m}$ )
- High refractive index
- Low losses

Some advantages for the bundle fabrication could be obtained using a cladding material with features such as:

- Low refractive index
- High optical attenuations across the Mid-IR
- Low Young modulus

The high optical attenuations of the cladding material allow to minimize the cross talk between individual cores while its low Young modulus provides flexibility to the overall structure. Furthermore, the high index contrast between the core and the cladding allows for a strong electromagnetic field confinement inside the low loss core. This strategy ensures practical Mid-IR transmission of low order optical modes for thermal imaging. The materials used in the present work have these characteristics. In fact, the core and the cladding materials were in chalcogenide Vitron IG3 glass and FEP polymer respectively.

### 2.1 Core Material: Chalcogenide Vitron IG3

As core material we chose the chalcogenide Vitron IG3 glass  $\text{Ge}_{30}\text{As}_{13}\text{Se}_{32}\text{Te}_{25}$  which is a commercial IR transmitting glass provided by Vitron (Schott). This glass has large transmission spectrum (2 - 12  $\mu\text{m}$ ), high refractive index (2.832 at 2  $\mu\text{m}$ ) and it is thermally stable. The refractive index  $n$  of Vitron IG3 glass as a function of wavelength is shown in Figure 1 (Vitron IG3, 2014). Vitron IG3 glass exhibits a glass transition temperature ( $T_g$ ) at approximately 275  $^\circ\text{C}$  (Vitron IG3, 2014). In order to measure the Vitron IG3 glass attenuations the cut-back method was applied on an uncladded Vitron IG3 glass fiber of 240  $\mu\text{m}$  of diameter. The uncladded Vitron IG3 glass fiber was obtained by drawing a Vitron IG3 glass rod of 12 mm of diameter. 39 transmission measurements were done and each cut was of 10 cm. The transmission of the uncladded Vitron IG3 glass fiber was measured by using the ARCOptix Mid-IR FTIR spectrometer. It has a Mercury Cadmium Tellurite (MCT) detector that covers a wavelength

range between 2 and 6  $\mu\text{m}$  (ARCOptix FT-IR Rocket data sheet, 2015). The Thorlabs SLS202L tungsten light source (wavelength range: 450 to 5500 nm) that emits IR light was used. Its emission is similar to a black body radiator at 1900 K (Stabilized Tungsten Light Sources, 2017). By using FC/PC connectors, one of the two ends of the fiber was connected to the Thorlabs SLS202L tungsten light source whereas the other end of the fiber was connected to the FTIR spectrometer. The uncladded Vitron IG3 glass fiber attenuations in dB/m measured using FTIR spectrometer are shown in Figure 2.

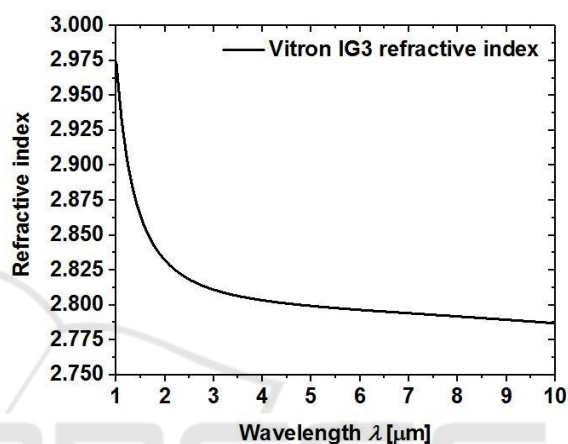


Figure 1: Refractive index of Vitron IG3 glass at different wavelengths provided by Vitron (Vitron IG3, 2014).

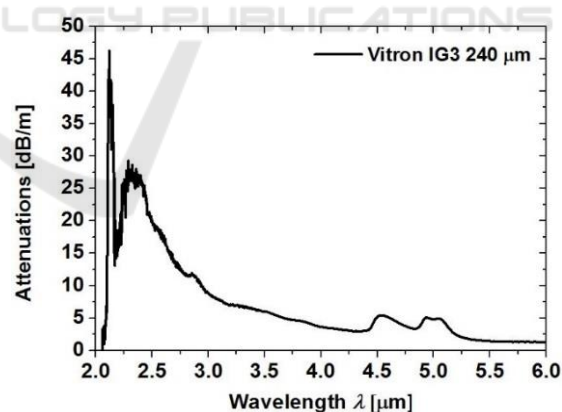


Figure 2: Vitron IG3 glass attenuations measured using FTIR spectrometer on an uncladded fiber of 240  $\mu\text{m}$  of diameter.

According to Snopatin *et al.* (2009), the functional groups  $[\text{OH}]^-$  and GeH absorb at 2.92 and 4.95  $\mu\text{m}$  respectively. The bands that appear at 2.32 and 4.52  $\mu\text{m}$  are attributed to SeH bond vibration (Snopatin, 2009). As the wavelength increases, the attenuations decrease (Figure 2); the uncladded Vitron IG3 glass

fiber displays typical loss values of 5 dB/m for wavelength ranging from 3 to 6  $\mu\text{m}$ . Between 2 and 3  $\mu\text{m}$  the uncladded fiber presents loss higher than 10 dB/m.

## 2.2 Cladding Material: Fluorinated Ethylene Propylene (FEP)

As cladding material, we chose the FEP polymer. It has similar chemical and electrical properties as the Teflon PTFE, however it is thermoplastic; the latter property allows to draw it into a fiber, while its low Young modulus allows to realise flexible fibers or bundles. Moreover, FEP polymer has a low refractive index ( $n=1.341$ ) (FEP Handbook). Figure 3 shows the FEP polymer attenuations in dB/m unit measured on a 0.86 mm thick sample using a Varian 670 FTIR spectrometer.

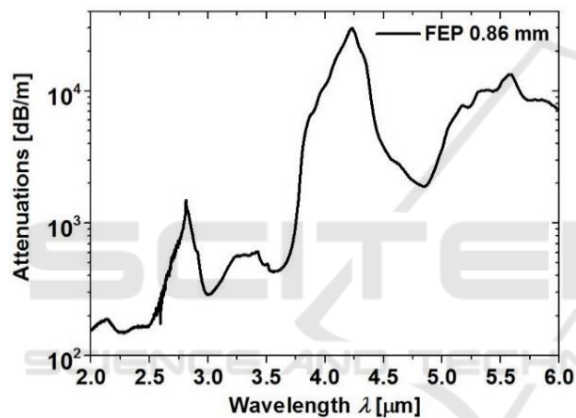


Figure 3: FEP attenuations measured using FTIR spectrometer on a sample 0.86 mm thick.

From Figure 3 it is possible to notice that the FEP polymer optical losses are high, typically above 1000 dB/m in the wavelength range between 4 and 6  $\mu\text{m}$ . According to Galante *et al.* (2010), the absorption at 4.23  $\mu\text{m}$  is due to the  $CF_2$  and the band at 5.57  $\mu\text{m}$  is due to terminal double bonds  $-CF=CF_2$  in the polymer chain.

## 2.3 Bundle Fabrication

A chalcogenide bundle with 1200 fibers was manufactured by using the stack and draw technique. The fibers were made with Vitron glass IG3 core and FEP polymer cladding. A Vitron IG3 glass preform of 12 mm of diameter was inserted in FEP polymer tube with external diameter equal to 14 mm and then placed into the drawing tower furnace under dried Ar atmosphere. Approximately 170 meters of fibers of

$300 \pm 8 \mu\text{m}$  in diameter were drawn at a speed of 2.1 m/min. This substantially high diameter variation is attributed to bubbles in the FEP polymer cladding. The Vitron IG3 glass appears to be crystal free and pristine. After the fiber fabrication, a stack of 1200 fiber sections, 120 mm long each, was realised and then it was inserted in an additional FEP tube with external diameter equal to 14 mm. This preform was drawn into two different fiber bundles of 1.1 and 0.675 mm of outer diameter, corresponding to individual core diameter of 22  $\mu\text{m}$  and 13  $\mu\text{m}$ , respectively. The overall yield was about 6 meters in length. Following fabrication, the fiber bundle was cut into sections of various lengths, ranging from 95 cm to 123.5 cm, to be characterized individually. Thermal images of a heating element were performed by using the fiber bundles and their attenuations were measured.

## 2.4 Bundle Characterization

In order to optimize the signal transmission, the ends of the fiber had first to be polished. This was achieved using a special jig designed in-house. The polishing procedure was carried out using a Logitech PM5 machine. Figures 4 and 5 show the optical micrographs of polished bundles of 22  $\mu\text{m}$  and 13  $\mu\text{m}$  in core diameter by using a Nikon Eclipse microscope. Overall, in the bundle structure the fibers are orderly stacked as in the original preform. A few pixels are missing or slightly out of position but further improvements are readily achievable by further increasing the density of the original preform. Qualitative thermal imaging assessments were carried out with a 1.15 m long Vitron IG3 fiber bundle, as follows.

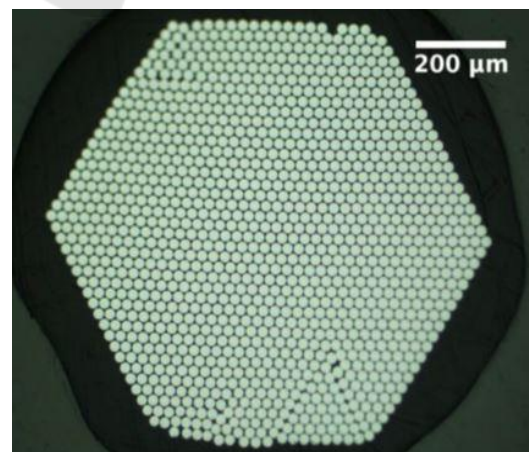


Figure 4: Vitron IG3 fiber bundle 22  $\mu\text{m}$  core micrography (10X).

A rectangular heating element, shown in the inset of Figure 6 was imaged on the input of the Vitron IG3 fiber bundle. Then, the output of the fiber bundle was imaged by using a thermal camera Xenics Onca-MWIR with InSb detector, which operates in a selected wavelength range between 3.6 and 4.9  $\mu\text{m}$  due to a filter. The images were focused by using chalcogenide lenses with antireflection coating. Figure 6 shows that for a heater temperature  $T=115\text{ }^\circ\text{C}$  the fiber bundle 1.15 m long transmits the infrared radiation. As one can see on the heating element image, the edges are sharp and well defined. Figure 7 shows that the minimum heater temperature for which we could obtain a clear image is for  $T=80\text{ }^\circ\text{C}$ . In fact, in order to transmit infrared radiation for a heater temperature lower than  $80\text{ }^\circ\text{C}$  the bundle attenuations must be decreased by purifying or by changing the core material. A metal target with inscribed letters was placed between the heating element and the input of the bundle in order to investigate the bundle resolution (Figure 8); the image shows that the resolution of the bundle is not yet satisfactory as some of the letters are not well transmitted and do not appear clearly. For this reason, in a future fabrication the resolution will be increased from 1200 to 3600 pixels.

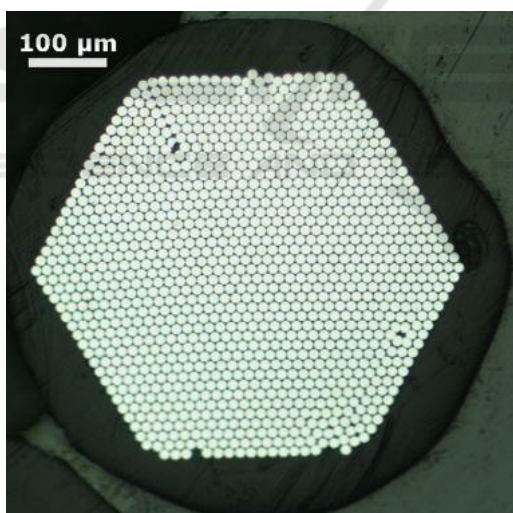


Figure 5: Vitron IG3 fiber bundle 13  $\mu\text{m}$  core micrography (10X).

The Vitron IG3 fiber bundle attenuations were measured using the cut-back method. 4 transmission spectra were measured by using the ARCOptix Mid-IR FTIR spectrometer and each cut was of 20 cm. Two different core diameters were investigated. For each core diameter two sets of cut-back measurements were carried out on two distinct bundle lengths, respectively in order to analyse the reproducibility of the measurements (Table 1).

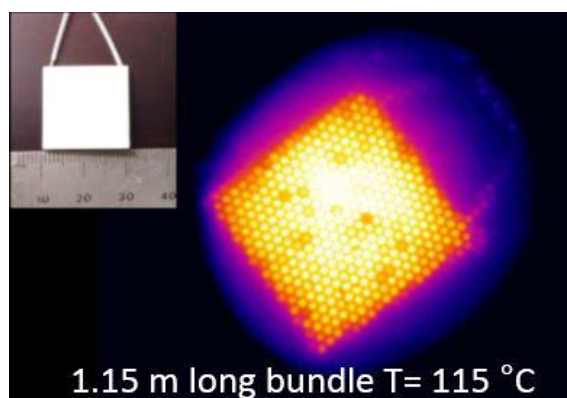


Figure 6: Thermal images of the heating element shown in the insert and held at  $T=115^\circ\text{C}$  by using a chalcogenide bundle of 1.1 mm of outer diameter.

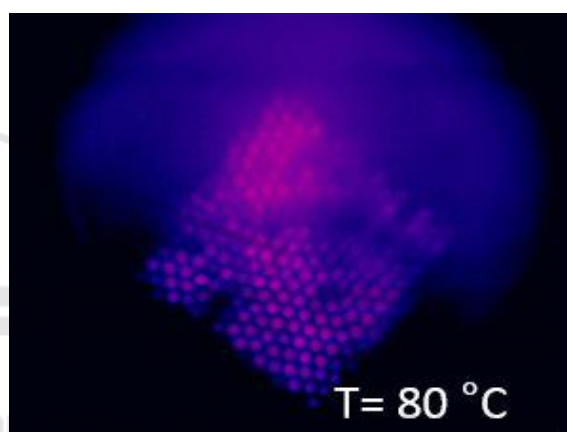


Figure 7: Thermal images of the heating element held at  $T=80^\circ\text{C}$  by using a chalcogenide bundle of 1.1 mm of outer diameter.

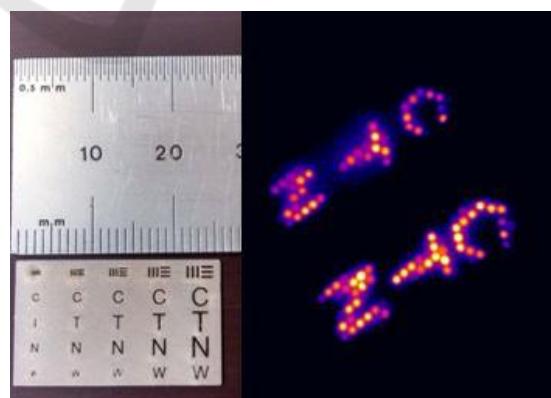


Figure 8: Thermal images of the heating element by using the metal target with inscribed letters shown in the inset to investigate the bundle resolution.

In the present work the 22  $\mu\text{m}$  core bundles labelled bundle 1 and bundle 2 in Table 1 and the 13  $\mu\text{m}$  core

bundles labelled bundle 3 and bundle 4 in Table 1 were compared in terms of attenuations. The Vitron IG3 fiber bundle losses calculated from the cut-back measurements are plotted in Figures 9-10.

Table 1: The bundle label and its corresponding core diameter.

Bundle	Core diameter [ $\mu\text{m}$ ]	Initial length [cm]
1	22	123.5
2	22	100.5
3	13	101
4	13	95

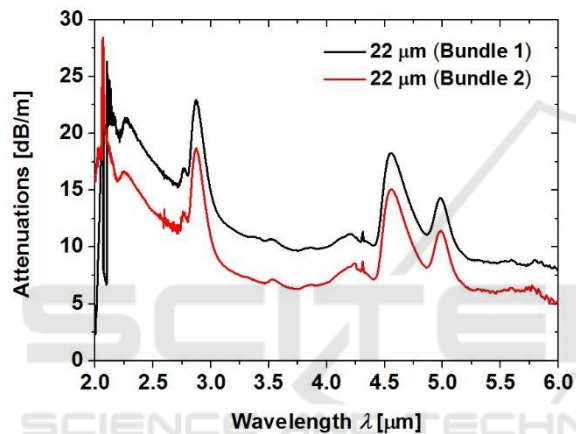


Figure 9: Attenuation of bundle 1 (black curve) and attenuation of bundle 2 (red curve).

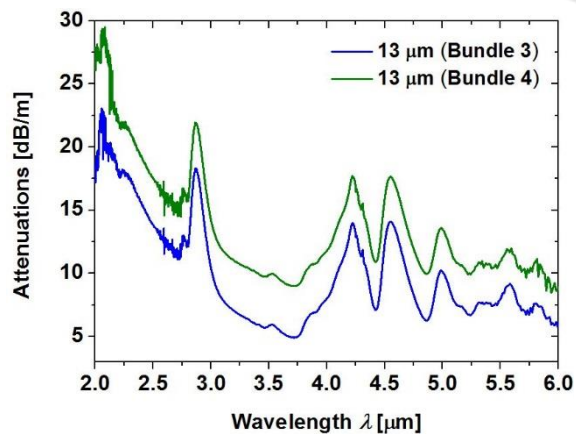


Figure 10: Attenuation of bundle 3 (blue curve) and attenuation of bundle 4 (green curve).

The attenuations for the Vitron IG3 fiber bundles of equal diameter are not the same. This is due to an error in the losses measurements induced from the

polishing quality and from the bundle coupling with the tungsten light source and the FTIR spectrometer. This error is  $\pm 1$  dB/m. A FTIR spectrum was calculated by averaging spectra of bundles with the same diameters. Figure 11 reports the losses of the Vitron IG3 uncladded fiber and the mean from a series of two spectra at 22  $\mu\text{m}$  and 13  $\mu\text{m}$  core diameter. The fiber bundle with 13  $\mu\text{m}$  core diameter presents two more pronounced peaks: at  $\lambda = 4.23$   $\mu\text{m}$  due to the  $CF_2$  absorption in the FEP and at  $\lambda = 5.57$   $\mu\text{m}$  due to terminal double bonds  $CF=CF_2$  in the FEP chain (Galante, 2010).

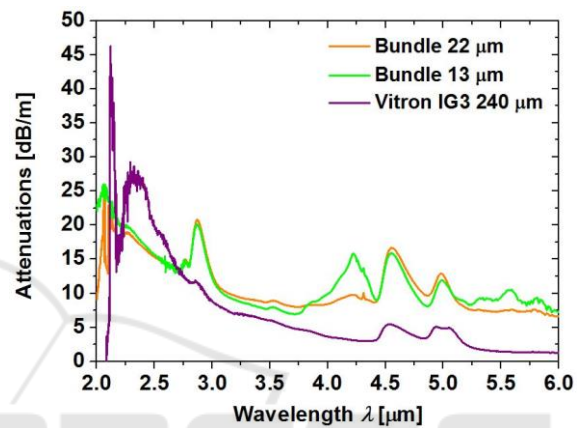


Figure 11: Bundles (orange and green curves) and Vitron IG3 glass uncladded fiber (violet curve) losses.

It is clear that the bundle losses are higher than the Vitron IG3 glass uncladded fiber due to the high cladding attenuations. The bundle losses are of the order of 10 dB/m in the wavelength range between 3 and 6  $\mu\text{m}$ . This loss value is high but still compatible with meter length applications. In the wavelength range between 2 and 3  $\mu\text{m}$  the fiber bundle presents higher attenuations. The peak at a wavelength of  $\lambda = 2.32$   $\mu\text{m}$  in the IG3 uncladded fiber attenuation spectrum is more pronounced than for the bundle spectra; this could be related to an impurity absorption from the uncladded fiber that is unprotected because it has no cladding. In Figure 11 it is shown that the attenuations of the two bundles (13  $\mu\text{m}$  and 22  $\mu\text{m}$ ) are almost comparable. These results give us some information for future work; the Vitron IG3 fiber bundle has high attenuations (10 dB/m) in fact it will be useful to use a chalcogenide glass with lower losses for future bundle fabrication to decrease the overall attenuations. The effect of the fiber diameter on the fiber attenuations was also investigated with a modelling study.

### 3 MODELLING OF OPTICAL FIBERS

The modelling study has been performed by using Comsol Multiphysics 5.2, which is a software for modelling and simulating Multiphysics problems (COMSOL Multiphysics, 2017). Comsol Multiphysics is based on the Finite Element Method (FEM) (Rahman, 2013).

#### 3.1 Modelling

The study of the modes propagation in an optical fiber made of Vitron IG3 glass core and FEP polymer cladding was performed by using the Finite Element Method (FEM). Five different scenarios were investigated by changing the core diameter to the following values: 9, 13, 15, 19 and 25  $\mu\text{m}$ . The attenuation effects in dB/m across every single fiber were calculated from the imaginary part of the complex propagation constant. The cladding diameter was fixed to 40  $\mu\text{m}$ . A Perfectly Matched Layer (PML) was applied to the fiber geometry to avoid any reflection of the electric and magnetic fields (Berenger, 1994). In Comsol, the PML diameter was fixed at 60  $\mu\text{m}$  and its parameters, i.e. the scaling factor and the curvature parameter, were set to 4 and 2 respectively. The fiber model was studied for three different wavelengths: 3  $\mu\text{m}$ , 4  $\mu\text{m}$  and 5  $\mu\text{m}$ . The real part of the complex refractive index  $n$  of the Vitron IG3 glass was loaded from the Comsol material library and its behaviour is shown in Figure 1. The extinction coefficient  $k$  of the Vitron IG3 glass was calculated from the FTIR loss measurements (Figure 2). For what concerns FEP polymer cladding material, the real part of the refractive index ( $n$ ) was set to 1.341. The extinction coefficient  $k$  of the FEP polymer was calculated from the FTIR loss measurements (Figure 3). A mesh with 55028 elements was used for this model. Considering the range of temperature of interest and the sensitivity of the thermal camera, an arbitrary loss value of 20 dB/m was considered. As first approximation, the overall losses of the Vitron IG3 glass core and FEP polymer cladding fiber were calculated from the average attenuations of the modes that have losses less than 20 dB/m. Figure 12 shows the results obtained, where it is clear that the fiber losses simulated decrease when increasing the core diameter. The modelling study show that the loss difference between bundles of 13 and 25  $\mu\text{m}$  core diameter is of the order of 1 dB/m. This observation suggests that it should be possible to develop a fiber bundle with an even smaller core size, without a

substantial increase in loss. The difference in terms of attenuations between the FEM simulations and the experimental results are due to two approximations. Firstly, for the modelled loss calculation we have considered the average attenuations of the modes that have losses less than 20 dB/m. Secondly, the bundle coupling with the tungsten lamp and FTIR spectrometer as well as the polishing quality influence the experimental results, with an error of  $\pm 1$  dB/m on the measurements. In order to improve the losses calculation in the modelling study, a method that takes into account the individual mode profile is undergoing.

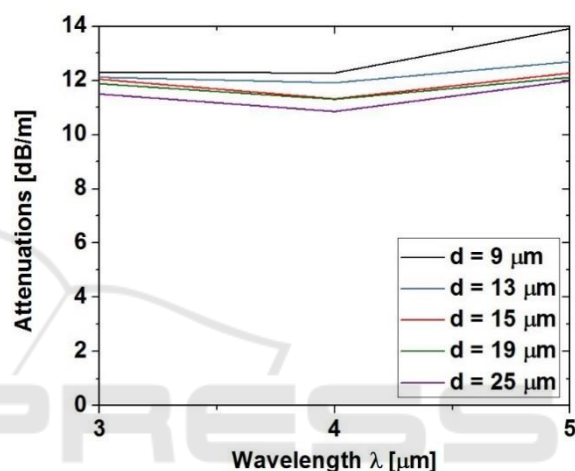


Figure 12: Average losses at different core diameters calculated by using Comsol Multiphysics: core diameter equal to 9  $\mu\text{m}$  (black curve), core diameter equal to 13  $\mu\text{m}$  (blue curve), core diameter equal to 15  $\mu\text{m}$  (red curve), core diameter equal to 19  $\mu\text{m}$  (green curve) and core diameter equal to 25  $\mu\text{m}$  (violet curve).

### 4 CONCLUSIONS

The stack and draw method was applied to achieve two flexible coherent Mid-IR chalcogenide bundles of 1.1 and 0.675 mm of diameter. The Vitron IG3 fiber bundle attenuations were measured using the cut-back method. The results obtained from this study have highlighted that the Vitron IG3 fiber bundle presents high losses (10 dB/m), but its structure is regular and the pixels are orderly stacked. The attenuations measured for the different core diameters (13 and 22  $\mu\text{m}$ ) were comparable. Thermal images show that a 1.15 m long bundle allows thermal imaging of objects at temperature higher than 80  $^{\circ}\text{C}$ . In fact, for a target at temperature equal to 115  $^{\circ}\text{C}$  the Vitron IG3 bundle (1.15 m long) transmits well the IR radiation and the target contours are well defined

and sharp. The behaviour of a chalcogenide fiber losses for different diameters was simulated by using the FEM. Results obtained from the modelling study also give an indication of the influence of the core size in the fiber attenuations. The typical difference between the loss of the 13 and 25  $\mu\text{m}$  core diameter fiber is only of 1 dB/m. This opens the possibility to achieve a new chalcogenide fiber bundle with even smaller core diameter and without substantial increase in optical losses. It is then possible to include a higher number of pixels (from 1200 to 3600) while maintaining the bundle outer diameter small enough to ensure mechanical flexibility, which will be the focus of the future work.

d2ea04f972b3-2DD86186-AF3B-B06B-E3D88182825A3929/SL5201L\_M-Manual.pdf (Accessed: 2 June 2017).

Vitron IG3, 2014. Available at: <http://www.vitron.de/datasheets/VITRON\%20IG-3\%20Datenblatt\%20Juni\%202014\%20.pdf> (Accessed: 19 December 2016).

Zhang, B., Zhai, C., Qi, S., Guo, W., Yang, Z., Yang, A., Gai, X., Yu, Y., Wang, R., Tang, D., Tao, G., Luther-Davies, B., 2015. *High-resolution chalcogenide fiber bundles for infrared imaging*, Optics Letters 40 (19), pp. 4384-4387.

## REFERENCES

ARCOptix FT-IR Rocket data sheet, 2015. Available at: <http://www.arcoptix.com/pdf/Data%20Sheet%20-%20Arcoptix%20FTIR%20Rocket.pdf> (Accessed: 13 February 2017).

Berenger J.P., 1994. *A Perfectly Matched Layer for the Absorption of Electromagnetic Waves*, Journal Of Computational Physics 114, pp. 185-200.

Chenard, F., Alvarez, O., D. Gibson, D., Brandon Shaw, L., Sanghera, J., 2017. *Mid-Infrared Imaging Fiber Bundle*, SPIE 10181, (2017).

COMSOL Multiphysics, 2017. Available at: <https://www.comsol.com/comsol-multiphysics> (Accessed: 11 April 2017).

FEP Handbook. Available at: [http://www.rjchase.com/fep\\_handbook.pdf](http://www.rjchase.com/fep_handbook.pdf), (Accessed: 19 December 2016).

Galante, A.M.S., Galante, O.L., Campos, L.L., 2010. *Study on application of PTFE, FEP and PFA fluoropolymers on radiation dosimetry*, Nuclear Instruments and Methods in Physics Research 619, pp. 177-180.

Gopal, V., Goren, A., Gannot, I., 2004. *Coherent hollow-core waveguide bundles for infrared imaging*, Opt. Eng. 5 (43), pp. 1195-1199.

Infrared Detectors, 2017. Available at: [http://www.hamamatsu.com/resources/pdf/ssd/infrared\\_kird0001e.pdf](http://www.hamamatsu.com/resources/pdf/ssd/infrared_kird0001e.pdf) (Accessed: 10 May 2017).

Nishii, J., Yamashita, T., Yamagishi, T., Tanaka, C., Sone, H., 1991. *Coherent infrared fiber image bundle*, Applied physics letters 59 (21), pp. 2639-2641.

Rahman, B. M., Agrawal, A., 2013. *Finite Elements Modeling Methods for Photonics*, Artech house.

Rave, E., Nagli, L., Katzir, A., 2000. *Ordered bundles of infrared-transmitting AgClBr fibers: optical characterization of individual fibers*, Optics Letters 25 (17), pp. 1237-1239.

Snopatin, G.E., Shiryayev, V.S., Plotnichenko, V.G., Dianov, E.M., Churbanov, M.F., 2009. *High-Purity Chalcogenide Glasses for Fiber Optics*, Inorganic Materials 45 (13), pp. 1439-1460.

Thorlabs. *Stabilized Tungsten Light Sources*, 2017. Available at: <https://www.thorlabs.de/drawings/b291>